Delta J. Sci. 2008, 32: 32-47 GEOLOGY

Primary uranium mineralization in sheared pegmatite of Wadi El Regita, South Sinai, Egypt.

Amer H.A. Bishr *, Said A. Azzaz**, Hassan M. Sherif* and Ibrahim E. El-Aassy*
* Nuclear Materials Authority, P.O.Box 530, Maadi, Cairo, Egypt.
** Department of Geology, Faculty of Science, Zagazig University, Zagazig, Egypt.

(Received: 7 March 2007)

Abstract: An important sheared pegmatite zone is hosted by the monzogranite of Wadi El-Regita area, south Sinai. This shear zone has an elongated shape with N 80o W trend and includes numerous highly altered spots. It is considered as the highest measured radioactive shear zone recorded in the area.

Based on field ground γ-ray spectrometric survey of the sheared pegmatite zone, 4 contour maps were compiled for total count (Tc), eU, eTh and eU/eTh ratio. The pegmatite shear zone is characterized by high levels of radiometric measurements especially along its strike. The obtained maps exhibit the presence of three main anomalies associated with the highly altered spots and mostly due to the presence of radioactive minerals e.g. brannerite, pitchekite, davidite and uraninite minerals, which are recorded for the first time in Sinai by the first author (Bishr, 2007).

The different minerals had been identified based on their radioactive and physical properties as well as X-ray diffraction (XRD) and Scanning Electron Microscope (XL30-ESEM, Philips) attached with EDAX unit. The ESEM analyses indicate the presence of brannerite, orthobrannerite, petscheckite, liandratite, uraninite, pyrochlores and columbites minerals. The average uranium contents of all the studied primary minerals grains vary from 12.73 to 82.87 wt%. Overall, Ce was the most abundant LREE in these grains. The Ce contents vary from 1.1 to 6.19 wt% and Nd varies from 0.15 to 2.35 wt%.

The major factors controlling the distribution of uranium mineralization within the studied sheared pegmatite are fracture system developed through the zoned pegmatite body during the course of the hydrothermal solutions migrated from deeper source through the structural weaknesses of the shear zone.

Introduction and geology.

El-Regita area is located to the northeast of the Katherine Mountain between latitudes 28° 38' 00"- 28° 35' 30" and Longitudes 34° 07' 15" - 34° 04' 15" (Fig.1) and can be reached via Wadi El-Sheikh. The geology of El-Regita area was previously described by some workers (e.g. Ibrahim (1991) and El-Ghawaby et al. (2000)). Ibrahim (op.cit.) concluded that the uranium and thorium mineralizations at the area were formed during two episodes. At the first, the thorium minerals with copper mineralizations were formed by hydrothermal solutions along WNW fault trend while the second is marked by the formation of uranium-bearing minerals along the younger N-S fault trend. El-Ghawaby et al. (op.cit.) concluded that the hydrothermal mineralization of Saint Katherine area has been ejected during the late stage of the intrusion of the granitic magma along inherited tensional Precambrian fabrics, which can be distinguished, based on fault-striate analysis, later dip-slip and strike-slip movements.

The investigated rock units are given in the geological map (Fig. 1). The detailed field studies of the exposed rock units revealed that the area is mainly covered by granodiorite and

monzogranite rocks. According to the field data, the monzogranite is highly jointed with predominant NE-SW and NW-SE trends. In addition, the N 80° W trending shear zone is observed in the monzogranite outcropping at western sides of Wadi El-Regita, this shear zone cuts through a zoned pegmatite body. The sheared pegmatites are marked by intensive closely-spaced fractures marked by striations, steps and crenulations along their planes due to the relative movements of the fracture walls relative to one another. Also, the quartz of this zone is highly fractured and mylonitized due to the effect of shearing (Figs 2A and 3B).

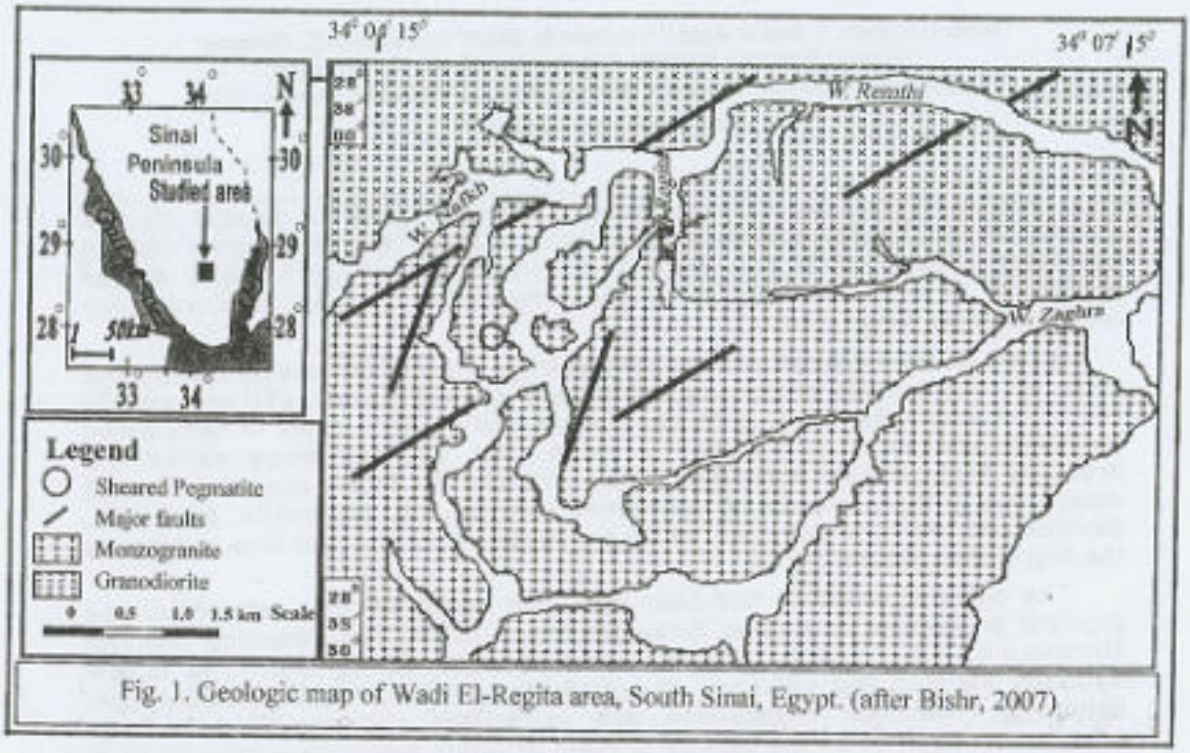

Fig. 1. Geologic map of Wadi El-Regita area, South Sinai, Egypt. (after Bishr, 2007)

The study zoned pegmatite has gradational contacts with its host monzogranite (Fig.2A) which indicates its later emplacement of magmatic evolution. It has the following zonal arrangement; wall zone, intermediate zone and core zone (Fig.2B). It is mainly composed of plagioclase, K-feldspars and quartz. The core zone is essentially composed of massive quartz and has sharp contact with the intermediate zone. The contacts between the other zones are gradational. The pegmatite body becomes mylonitized and cataclased due to the effect of the cross-cutting shear zone (80 - 100cm width). Some highly radioactive spots are detected along the shear zone and associated with weak hematitization and kaolinitization. Black coloured-uranium minerals (Fig.3.A and B) are encountered along the fissures associate the sheared pegmatite at the contact between wall zone and core zone. The black coloured grains show high radioactivity. The length of the highly radioactive area is about 15m, while the width reaches to 1m in different spots.

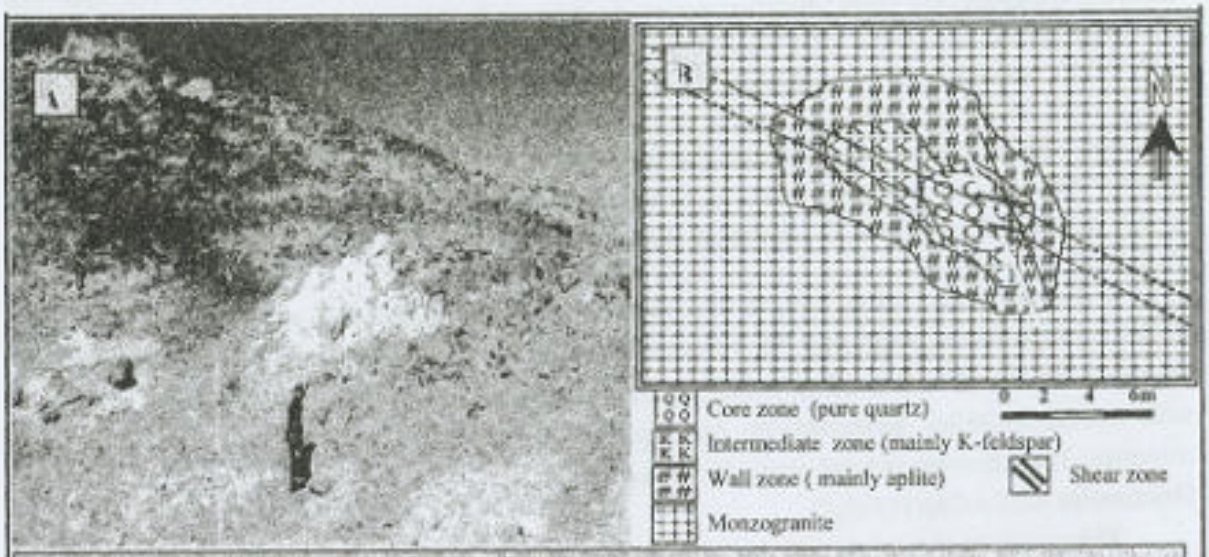

Fig. 2 (A): General view and (B): Schematic diagram showing the successive zones of the sheared pegmatite body. The first author stands as a scale.

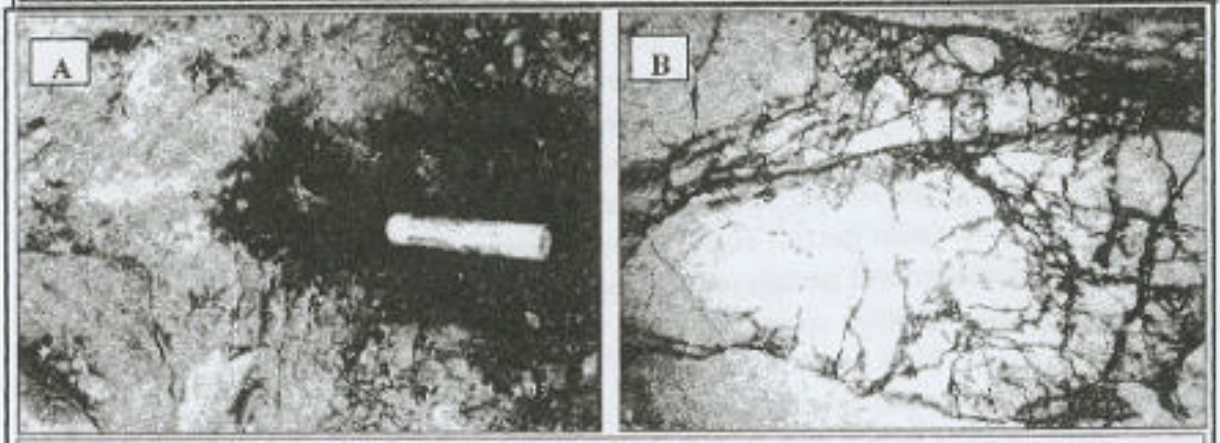

Fig. 3. A: Coarse grain of black coloured uranium minerals are encountered along the fissure cutting the pegmatite. **B.** Photomicrograph showing uranium minerals of the sheared pegmatite occur as filling fracture enrichment. X10 C.N.

MINERALOGY

This study deals with, and shed light on primary uranium minerals and their associations in sheared pegmatite of the study area. Uranium minerals are generally classified into two main groups, namely primary and secondary minerals. The terms primary and secondary should be used to describe the initially deposited and the alteration mineral, respectively. The reduced minerals are usually uraninite with or without association of rare earths elements and other actinide elements. Niobate, tantalite and titanate uranium minerals are also common as primary minerals (Smith, 1984).

Methodology

The anomalous samples, whether soft or hard, were collected and subjected to desegregation to facilitate the identification of all minerals, as well as the uranium-bearing minerals. Starting with crushing technique and the crushed product is screened. The fractions having grain size range from 0.125mm to 0.5mm were used in mineral investigation. The selected fraction subjected to heavy liquid separation using bromoform and methylene iodide

separation technique. The obtained heavy fractions were subjected and carefully investigated under the binocular stereo microscope in order to identify the different mineral crystals. The different minerals had been identified based on their radioactive and physical properties as well as X-ray diffraction (XRD) and Scanning Electron Microscope (XL30-ESEM, Philips) attached with EDAX microanalysis unit developments in high-pressure (low-vacuum). The analyses were carried out in the laboratories of the Nuclear Materials Authority, Cairo, Egypt. The ESEM, attached with EDAX unit, analyses indicates that the average uranium contents of all the studied primary minerals grains vary from 12.73 to 82.87 wt%. Overall, Ce was the most abundant LREE in these grains. The Ce contents vary from 1.1 to 6.19 wt% and Nd varies from 0.15 to 2.35 wt%.

The mineralized zone around the quartz core of the pegmatite is characterized by the presence of ilmenite, rutile and Ta, Nb-bearing uranium minerals. The Ta, Nb-bearing uranium minerals are found in this zone, including the recorded new minerals brannerite in association with orthobrannerite, petscheckite and liandratite, uraninite, pyrochlores and columbites minerals. The following is brief accounts on each mineral.

Brannerite $(U,Ca,Ce)(Ti,Fe)_2O_6$

Brannerite is the third most important reduced uranium mineral in that it occurs in many different types of deposits. Although it has been found in pegmatites, hydrothermal and sedimentary deposits it is always associated with uraninite and probably forms through reactions with uraninite and titanium phases (Smith (1984).

The XRD examination of the picked grains, which are obtained on heating to improve crystallinity, reveals the presence of brannerite in association with orthobrannerite and uraninite (Fig.4). The analyses of the same grains by the ESEM technique (Fig.5) shows that the main composition are Ti, U and Nb and some U is oxidized and replaced by Ca and Nb, while the Fe partially replaces Ti. Smith (op.cit.) concluded that, brannerite is nominally UTi_2O_6, but the U may be partially oxidized and partially replaced by Ca and rare earths. Fe may replace some of the Ti and partial hydration may occur and the formula of brannerite may be (U, Ca, RE)$(Ti,Fe)_2O_{6-8}(OH)_x$. Mock and Ohmoto (1997) concluded that the uraninites are associated with brannerite, rutiles and ilmenite grains of the Elliot Lake District, such associations may indicate these minerals formed by hydrothermal fluids.

Orthobrannerite, with a formula of $U^{4+}U^{6+}(Ti,Fe)_4O_{12}(OH)_2$ has been reported by the Peking Institute of Uranium Geology (1978). Uraninite was the only known U^{4+} minerals but recently the list now contains 11 species including brannerite. Orthobrannerite contain uranium in valance state higher than 4+ and less than 6+.

The studied brannerite (Fig.6) is mostly distinguished by brown to black colour, anhedral shape, non cleavage, diaphaniety opaque to sub translucent and the luster is resinous.

Petscheckite $[U,Fe\ (Nb,Ta)_2O_8]$ **and liandratite** $[U(Nb,Ta)_2O_8]$

Petscheckite and its alteration product liandratite have been reported from a granite pegmatite in Madagascar (Mücke and Strunz, 1978). It is identified by its X-ray powder pattern obtained on heated material. REE-bearing petscheckite was recently described through a granite pegmatite at Tiltvika, Nordland (north Norway) by Tomašić et al. (2004). It should be noted that, the total content of REEs nearly equals the content of uranium in the Tiltvika petscheckite.

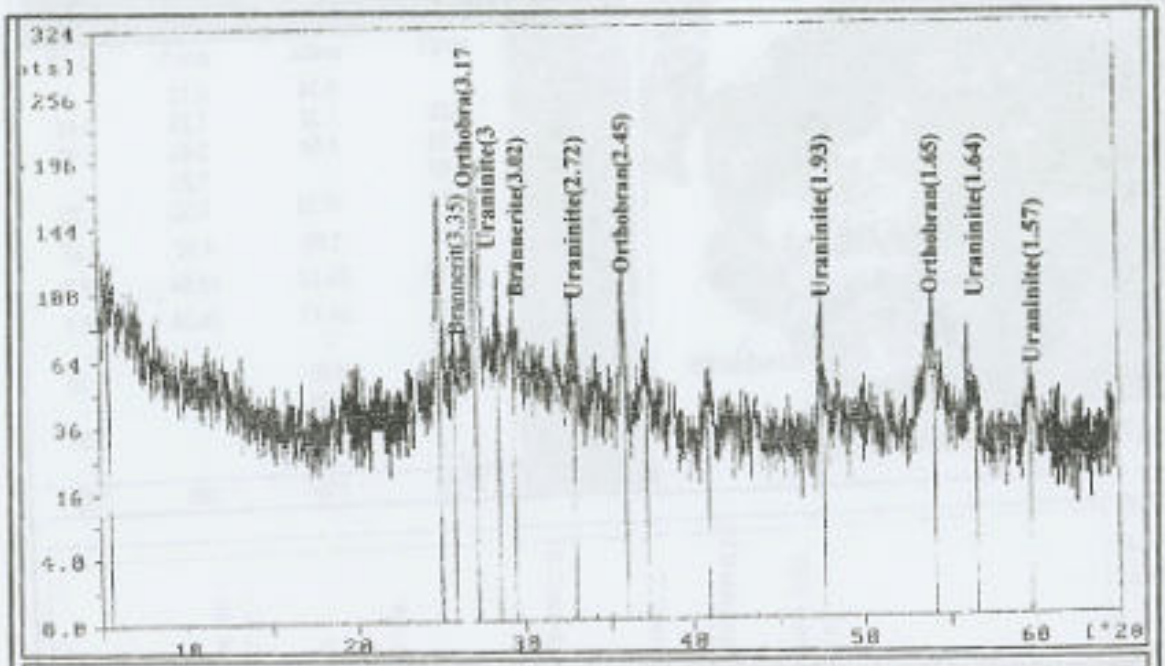

Fig. 4. XRD pattern of brannerite ASTM card No. (12-477), orthobrannerite and Uraninite ASTM card No. (5-550)

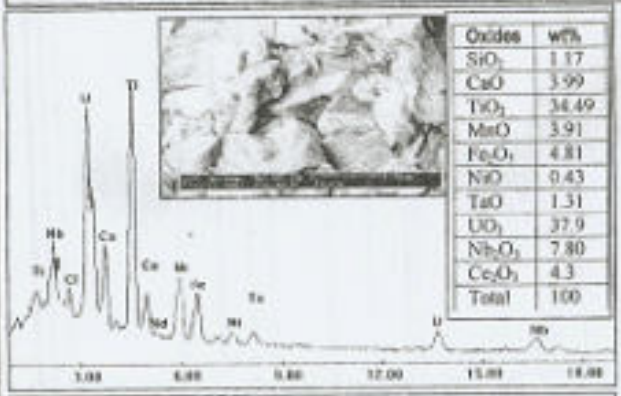

Oxides	wt%
SiO_2	1.17
CaO	3.99
TiO_2	34.49
MnO	3.91
Fe_2O_3	4.81
NiO	0.43
TaO	1.31
UO_2	37.9
Nb_2O_5	7.80
Ce_2O_3	4.3
Total	100

Fig.(5): BSE images showing photo and the chart of the analysed grains of brannerite mineral.

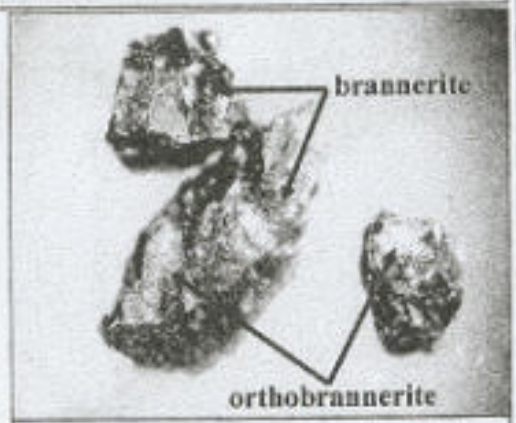

Fig.(6): Brannerite & orthobrannerite (64 X).

Liandratite mineral appears as an oxidation product (Fig.7) surrounding petscheckite, as closely associated phases, that identified by X-ray diffraction (XRD) Fig. (8). The ESEM examination of the petscheckite grains (Fig. 9A) reveals that minor amounts of Ca, K, and Mn were found in the related phase with petscheckite, that agree with Gregory et al. (1996) Table 1. Mücke and Strunz, 1978, concluded that $U(Nb,Ta)O_6$ arises through complete oxidation of uranium and iron, where nearly all Fe^{3+} ions have been removed from petscheckite. This process occurred in situ and only on the surface of petscheckite crystals, which are therefore epitaxially overgrown by liandratite. The agreement between our data (analysis) and those of (Mücke and Strunz, 1978) are quite good, the ESEM examination of the liandratite mineral (Fig. 9B) are enriched in CaO and Nb_2O_5 and appear as a coating of the petscheckite crystals, probably due to oxidation.

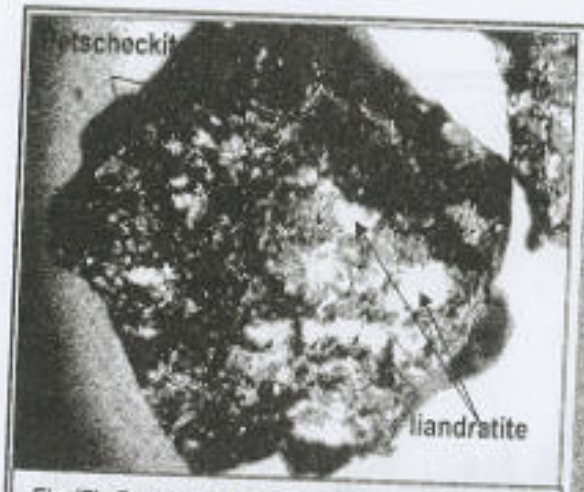

Fig.(7): Petscheckite & liandratite (64 X).

Table 1. Average analysis of the studied petscheckite (amS1) and (amS2) and liandratite (amL1) and (amL2)

Oxides	amS1	amS2	amL1	amL2
Al_2O_3	-	0.24	0.12	-
CaO	2.59	1.32	1.22	2.44
TiO_2	5.51	4.54	3.45	5.16
MnO	0.57	-	1.20	-
Fe_2O_3	8.12	10.33	4.32	1.70
Ta_2O_5	5.66	3.55	4.66	4.37
Nb_2O_5	27.50	25.12	46.54	37.0
UO_2	47.76	54.13	38.24	48.1
Nd_2O_3	0.06	-	-	-
K_2O	1.25	0.29-	0.25	0.59
ThO_2	-	0.25	-	-
Ce_2O_3	-	0.23	-	0.64
Y_2O_3	0.47	-	-	-
Total	99.53	100	100	100

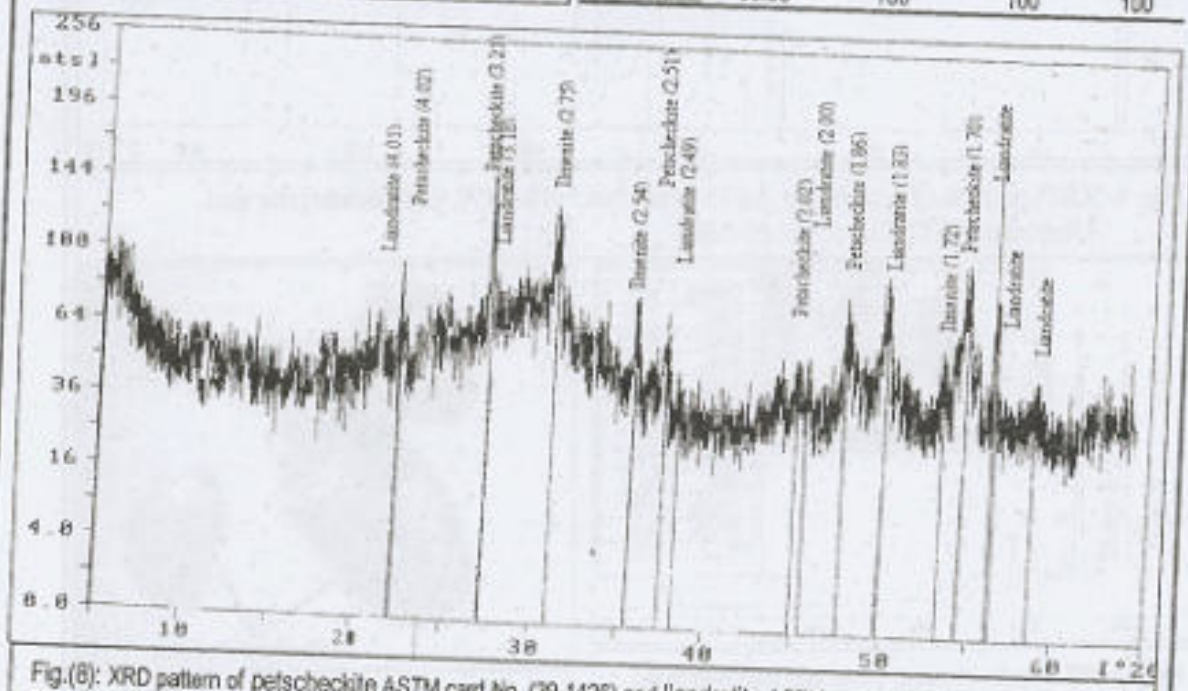

Fig.(8): XRD pattern of petscheckite ASTM card No. (29-1426) and liandratite ASTM card No. (29-1435) with ilmenite.

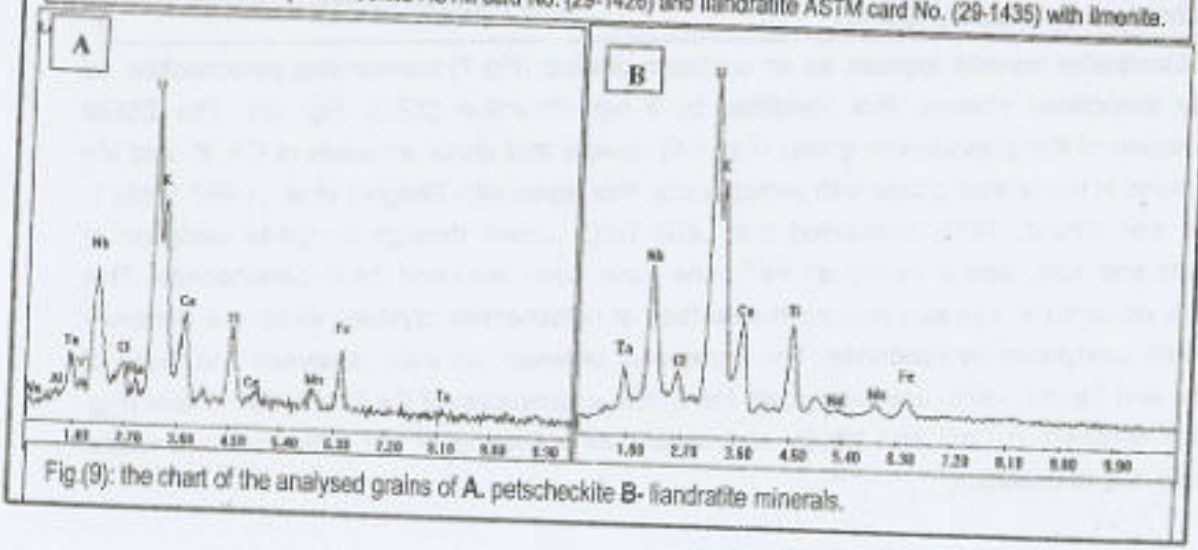

Fig.(9): the chart of the analysed grains of **A.** petscheckite **B-** liandratite minerals.

The analyses show low percent of Fe_2O_3 in liandratite which probably removed from the outer surface of the petscheckite to produce liandratite which has brownish yellow colour. Based on Dahlkamp (1979) and Smith (1984), petscheckite is one from the lowest valance state for uranium in nature i.e. 4+ (primary uranium minerals). Its tendency to partially oxidize to contain uranium in which the average valance state is definitely higher than 4+ but less than 6+ represented liandratite mineral. Petscheckite is distinguished by its anhedral shape, black colour, uncleavable, metallic luster and smoothly curving surfaces. While the main physical properties of petscheckite and liandratite are metamict, even though they occur as crystals, and heating is required to produce crystallinity.

Uraninite (UO_2) is the most abundant uranium mineral present in vein-type uranium deposits and the only commonly occurring U^{4+} mineral. Uraninite is easily identified by its X-ray diffraction pattern, and all UO_{2+x} show the same pattern, except for the changes in spacing due to composition Smith (1984). The studied uraninite occurs in the form of minute inclusions as disseminated particles associated with the other uranium minerals (brannerite, petscheckite, ashanite,..), rutiles and ilmenite grains. Such associations may indicate these minerals formed by hydrothermal fluids (Mock and Ohmoto, 1997).

The studied uraninite can be identified by both XRD and ESEM techniques. Fig. 10 shows uraninite associates brannerite orthobrannerite while Figure 11 and 13 showing uraninite associates ashanite and ilmenite minerals. Uraninite shows range of colours, from the usual brownish black variety with typical conchoidal fracture, to a grayish black and black variety resembling petscheckite, but is distinguished from brannerite and liandratite by its greasy luster. The study of uranium deposits is complicated by the susceptibility of uraninite to alteration and radiation damage, and because the effects of these processes are most evident at the nano- and micro- scale (Fayek et al., 2003).

Some uraninite grains are investigated by ESEM technique (Table 2 and Fig. 14 samples Nos. am5 and am5b), showing that the crystals contain an appreciable average content of Ca reach to 1.64%, Pb reach to 2.4%, and REE and Nb reach to 10.3%. The U percent fluctuated between 79.3% and 83.6% in different samples. Uraninite compositions in the samples are mostly non uniform. Analyses of uraninite grains and veins, that is, micro-analyses of volumes of uraninite between 5 and 10 mm in diameter, reveal that uraninite compositions, particularly U, Pb and Ca contents, vary not only from grain to grain within anyone sample regardless of which generation of uraninite it is, but even at the microscopic level within uraninite grains themselves. Pb and Ca have both substituted for U in the UO_2 cubic lattice in varying amounts across the uraninite veins and grains (Snelling, 1995). Frondel (1958) described two types of uraninite; pegmatite (magmatic) and hydrothermal types. Pegmatite uraninites commonly have ThO_2 = 2% or more while hydrothermal variety has less than 0.25% ThO_2. The available data (Table 2 and Fig. 14) reveal the presence of ThO_2 less than 0.1%. This may suggest the hydrothermal origin of this uraninite. The chemical composition of the studied uraninite illustrates that the percentage of UO_2 (79.3% - 83.6%) lies in the U range of uraninite supported by Heinrich, (1958) and Pb occurs as a radioactive decay product.

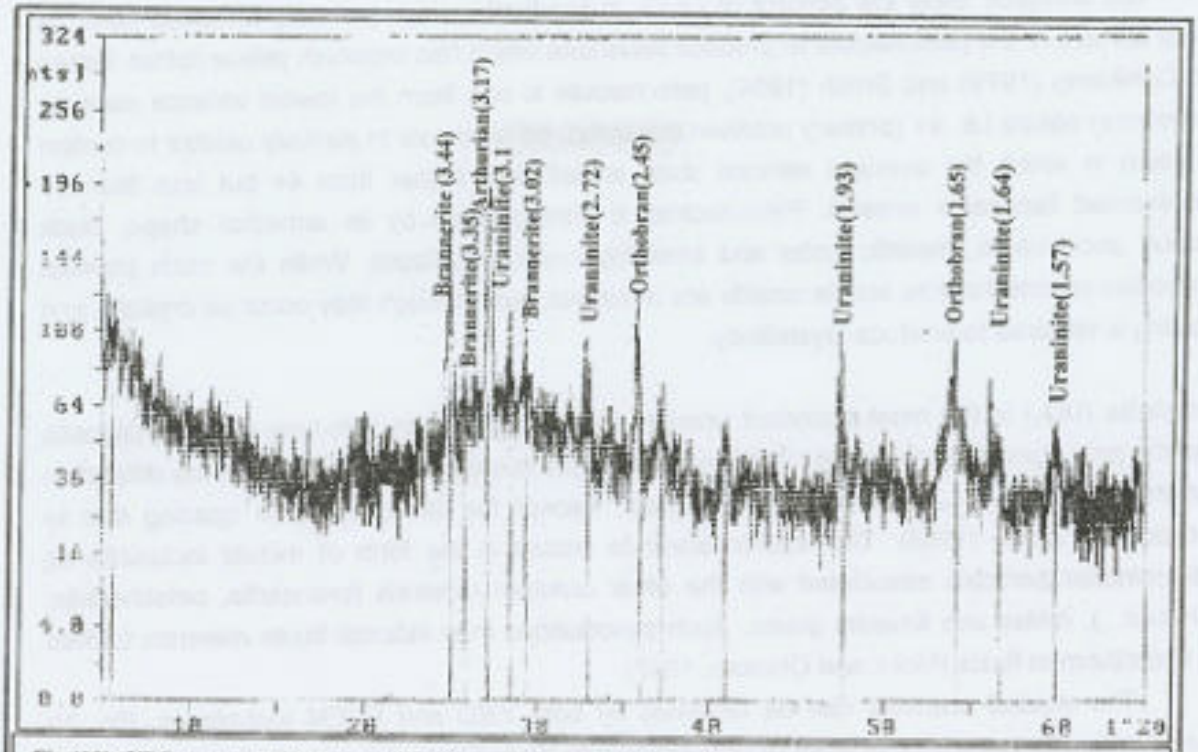

Fig.(10): XRD pattern of brannerite ASTM card No. (12-477), orthobrannerite and Uraninite ASTM card No. (5-550)

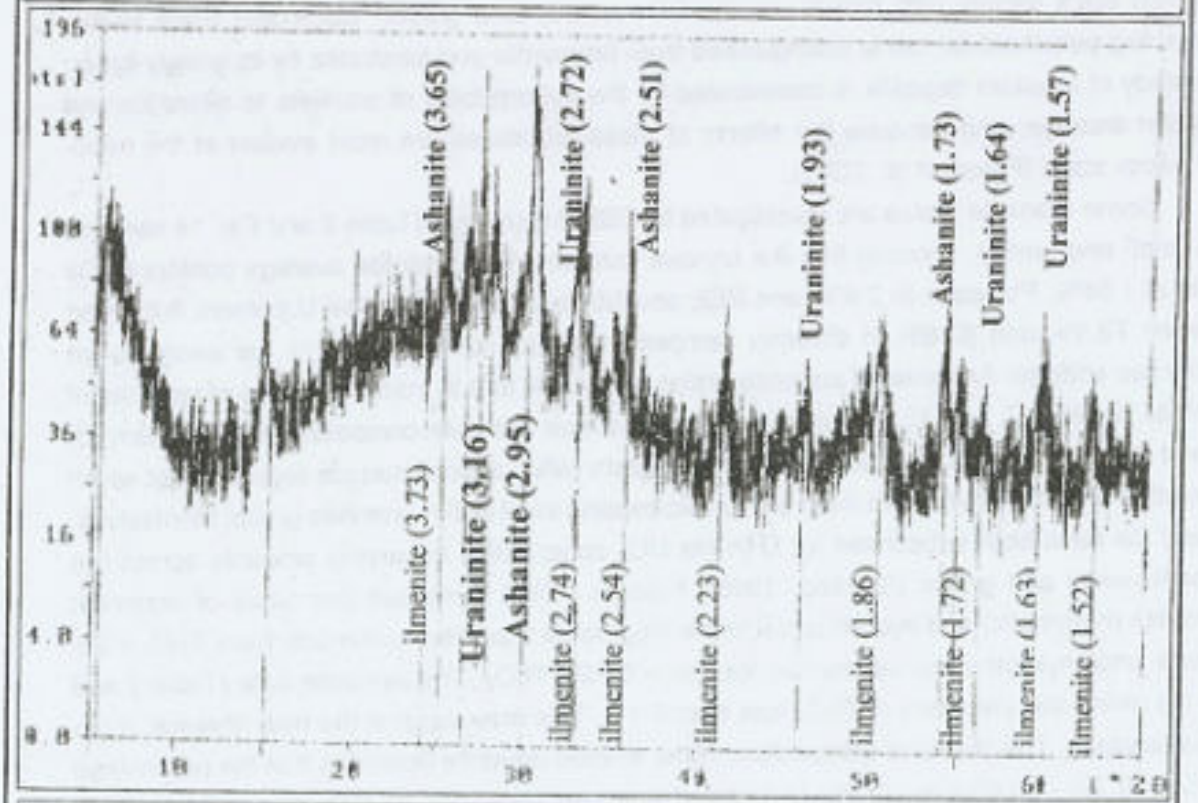

Fig.(11): XRD pattern of uraninite ASTM card No.(5-550), ashanite ASTM card No. (33-660), and ilmenite.

Table (2): Average chemical analysis of the studied uraninite (am5), (am5a) and (am5b)

Oxides	am5	Am5a	am5b	*Av.*
SiO_2	1.62	2.9	3.03	*2.52*
PbO2	0.43	1,6	2.41	*1.48*
CaO	1.58	1.7	1.64	*1.64*
MnO	-	0.1	-	*0.10*
Fe_2O_3	0.67	0.63	0.74	*0.68*
UO_2	83.6	80.46	79.3	*81.12*
Nb_2O_5	10.3	8.2	8.9	*9.13*
K_2O	0.55	0.41	0.54	*0.50*
ThO_2	-	0.1	0.1	*0.10*
Ce_2O_3	1.1	2.9	3.2	*2.40*
P_2O_5	0.1	0.1	0.1	*0.10*
Total	*99.9*	*99.8*	*100*	*99.77*

Fig.(12): Uraninite associates brannirite. (64X)

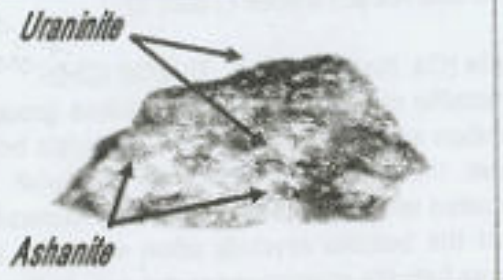

Fig.(13): Uraninite and ashanite (64X)

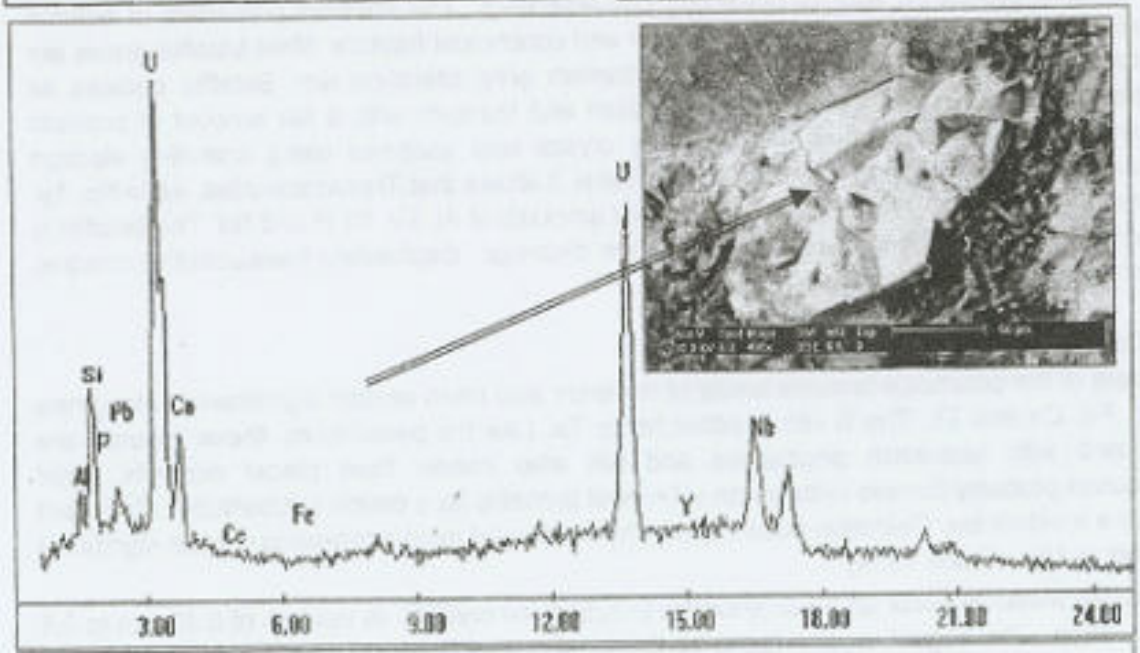

Fig.(14): BSE images and the chart of the analysed grains of uraninite minerals.

It is well documented in many uraniferous pegmatites allover the world (e.g Canada) that all uraninite and pitchblende grains contains Pb of radioactive origin. Ca is recorded to be associated with uraninite in Canada (Morton and Sassano, 1972). Si and Fe may also replace in variable amounts.

The studied uraninite occurs as small subhedral equidimensional crystals or in the form of narrow, irregularly shaped veinlets, associated with fracture rich in hematite. However, uraninite is absent at fractures free of hematitization, indicating the association of the formation of vein-type uraninite with hematitization process.

Uranium Niobates, Tantalates and Titanates

Uranium is commonly found in the rare-earth tantalates and niobates, but the valence states of the uranium are not well established, although many of these minerals probably formed with the uranium initially in the 4+ state, chemical analyses indicate that both 4+ and 6+ are present (Smith 1984). The description of identified minerals will be discussed below:

Pyrochlores have a general formula A2B2O6(O,OH,F), where U4+ (or U6+) occurs in the A site and B = Ta, Nb, Ti. The nomenclature of the pyrochlore series was discussed by Hogarth (1977). The master name refers to the dominant element in the B sit. Betafite refers to Ti, microlite to Ta and pyrochlore to Nb.

Pyrochlore minerals appear as network of veins or fissure filling of the sheared pegmatite by very bright colour (Fig.15). The data was obtained by (EDAX) unit, which refer to Nb predominantly Ti and Ta. U is the main constituent. Y, Ca and K are obviously reported, while Mn, Fe and Na are traces (Table 3).

Betafite (Ca, Na, U) (Ti, Nb, Ta)2O6 (OH).

The betafite subgroup of the pyrochlore group is defined by 2Ti ≥ Nb + Ta for the B-site cation population and compositional series exists between pyrochlore and betafite. (Hogarth 1977). In general, the studied betafite has yellowish brown colour and adamantine luster Fig(16). It associated with ashanite and clakeite minerals in the samples of sheared pegmatite area. The size of the betafite crystals allow detecting by separate XRD pattern (Fig. 17) after heating, because betafite specimens occur only in the metamict state, to reveal patterns and D-spacings compatible to those of betafite. This suggests that on heating there is almost a complete restoration of the lattice and its diffraction characteristics. The physical properties of betafite attain the black colour, earthy to metallic luster and conchoidal fracture. Most betafite grains are characteristically surrounded by a narrow brownish grey alteration rim. Betafite occures as inclusions contain high concentrations of niobium and titanium, with a fair amount of uranium and small amount of tantalum. The betafite crystal was analyzed using scanning electron microscopy (ESEM attached with EDAX unit), Table 3 shows that Ti predominates, while Nb, Ta, U, Ca and Pb are widely represented, with minor amounts of Al, Fe, Ni, P and Nd. The betafite is characterized by its yellowish brown colour, non cleavage, diaphaniety translucent to opaque, uneven fracture and adamantine luster.

U4+ Columbites-AB2O6

Members of the columbite-tantalite family of minerals also often contain significant U along rare earths, Fe, Ca and Th. The B site is either Nb or Ta. Like the pyrochlores, these minerals are associated with rare-earth pegmatites and are also known from placer deposits. Most compounds probably formed initially with U4+ most probably as a coupled substitution Ca2+ and U4+ for a trivalent ion. Oxidation occurs easily, however, and most specimens contain significant amounts of U6+ (Smith 1984).

Columbites minerals occur as black anhedral to subhedral crystals, in veinlets of 0.25 mm to 0.5 mm in width. The largest crystal found at the locality associated with uraninite and ilmenite minerals. It is translucent and has a reddish brown colour along the edges. The assignments of ashanite mineral pattern are detected, related to those minerals which are usually metamict and require heating to develop crystallinity.

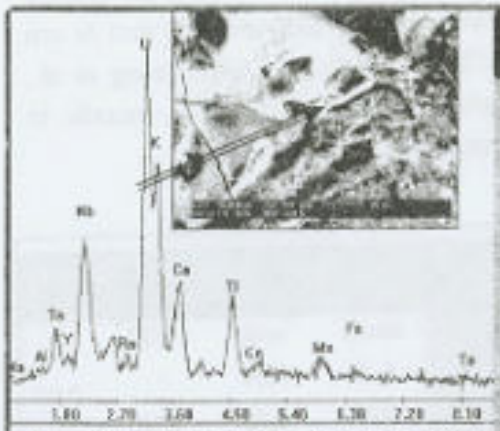

Fig.(15): BSE image showing photo image and the chart of the analysed

Fig.(16): Betafite and pyrochlore (64X).

Table 3. Average chemical analysis of the studied pyrochlore and betafite minerals.

Type	Pyrochlore				Betafite			
Oxide	amS	am4	amN	Av.	amM	am3	am8	Av.
Al_2O_3	-	1.37	0.43	**0.9**	-	1.84	1.74	**1.79**
SiO_2	1.4	7.35	-	**4.36**	3.31	12.9	2.70	**6.31**
CaO	3.67	4.79	5.08	**4.51**	7.04	5.42	6.63	**6.36**
TiO_2	5.5	8.56	6.44	**6.82**	17.2	,12.2	31.1	**20.2**
MnO	0.5	0.33	1.36	**0.75**	1.30	4.33	-	**2.82**
Fe_2O_3	0.9	2.27	0.66	**1.28**	3.94	1.98	3.23	**3.05**
NiO	-	0.91	-	**0.91**	-	0.80	1.43	**1.12**
Ta_2O_5	1.0	1.60	2.24	**1.61**	-	3.40	3.89	**3.65**
UO_2	47.3	45.4	50.6	**47.8**	44.4	29.2	19.3	**31.0**
Nb_2O_5	38.6	24.3	28.2	**30.4**	15.7	22.8	27.8	**22.1**
K_2O	2.1	2.16	2.42	**2.23**	3.85	1.15	-	**2.5**
ThO_2	-	0.68	-	**0.68**	-	3.23	-	**3.23**
Nd_2O_3	0.06	0.30	-	**0.18**	-	0.71	0.92	**0.82**
Ce_2O_3	-	-	0.80	**0.8**	1.43	-	-	**1.43**
Na_2O	-	-	0.37	**0.37**	0.87	-	-	**0.87**
Y_2O_3	-	-	1.26	**1.26**	-	-	-	
Total	100	100.	100.	**99.59**	99.3	100.	99.9	**99.7**

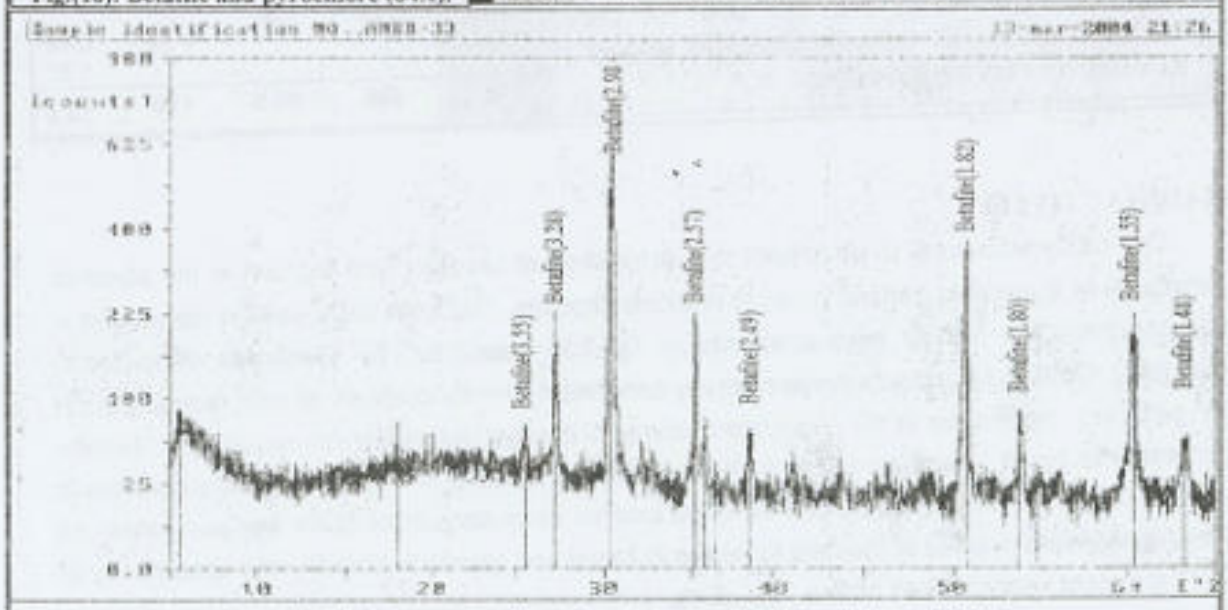

Fig. (17): XRD pattern of betafite minerals ASTM card No. (8-300).

The obtained XRD data for brown ashanite grains (Fig. 11) are associated with uraninite and ilmenite, separated from the samples of sheared pegmatite. The same samples were analyzed by ESEM for their elemental composition, backscattered electron images (Fig. 18). It

was found that, both the XRD data and ESEM spectra conforms to the composition of ashanite mineral, the charts of the analyzed grains and EDAX (Table 4. sample Nos. am2a, am2 and am42) indicate the presence of ashanite minerals, Nb, Ti, Ta, U and Mn are the main constituent with Nb predominantly Ti and Ta. REE, Ca and K are obviously reported, while Ni and Al are traces. The present ashanite is relatively enriched in Mn% in comparison with Zhang et al., (1980). The physical properties of ashanite appear as dark brown colour (Fig. 13), metallic to sub metallic luster, opaque diaphaneity and conchoidal fracture.

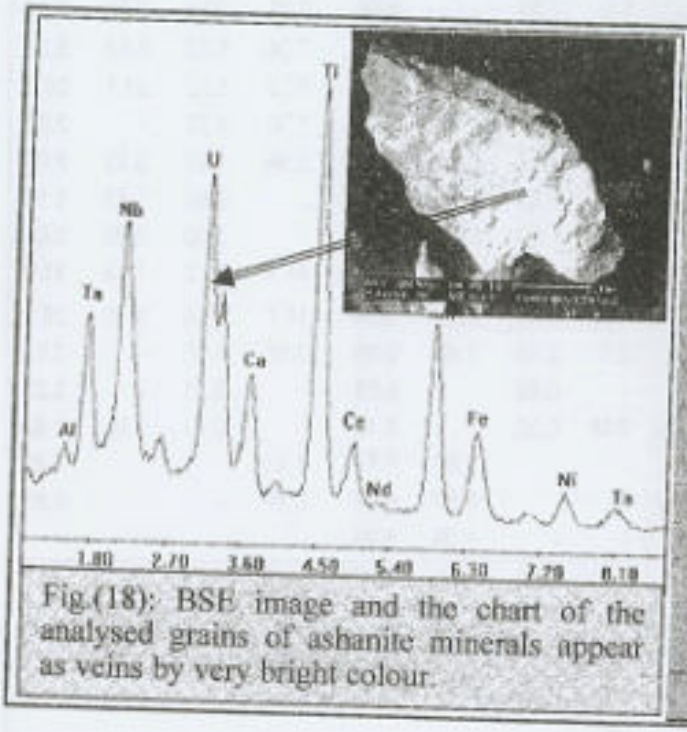

Fig.(18): BSE image and the chart of the analysed grains of ashanite minerals appear as veins by very bright colour.

Table 4. Analysis of the studied ashanite am2a, am2 and am42

Oxides	am2a	am2	am42	Av.
Al_2O_3	0.43	0.69	-	0.56
CaO	4.27	1.75	4.10	3.4
K_2O	1.10	0.55	-	0.8
TiO_2	14.31	11.18	16.05	13.8
MnO	10.73	7.15	15.56	11.1
Fe_2O_3	5.31	5.23	-	5.27
NiO	0.91	0.14	-	0.53
Ta_2O_5	18.85	23.22	18.05	20.0
UO_2	21.77	14.46	20.46	18.9
Nb_2O_5	22.19	33.97	24.49	26.9
Nd_2O_3	0.15	1.61	-	0.88
Ce_2O_3	-	-	1.37	1.37
Total	100	99.5	100	99.8

RADIOACTIVITY

This study was done to document the distribution of uranium and thorium in the sheared pegmatite as a possible general guide to uranium deposits. The instrument used in the ground γ-ray spectrometric survey measurements is GS-256 (designed by Geofyzika Brno-Czech Republic). Ground γ-ray spectrometric survey can detect directly contents of total radioactivity in Ur unit (Tc), potassium (K%), equivalent uranium content (eUppm) and equivalent thorium content (eTh ppm). Random grid is mainly used in the profiles. The interval between profiles is usually 5 meters. The area between the grids profiles were also checked for any anomalies. All the stations were marked in the field to be easily found and checked. Stability and consistency of the instrument was checked before field using.

The mean, standard deviation and median of eU and eTh concentrations for a sum of 125 gamma-ray spectrometry measurements of sheared pegmatite area are presented in Table 5. The area is generally characterized by high levels of radiometric measurements. From Table 5, the eU mean = 10.9 ppm, and the average eU/eTh ratio is 0.33. Whereas, the average eTh is 32.2 ppm. However, the eTh/eU equal 3.99. According to Stuckless, (1979) opinion, if the

thorium anomalies are accompanied by Th/U ratios greater than 5 uranium loss from the basement rock seems probably, but, the ratio is less than 5.

From the field observation and plotting the measurements, two separate high radioactivity spots are recorded (Fig. 19.A), which has radioactive measurements higher than 95 Ur. The distribution of the two anomalies on the map indicates an important structural trend controlling them through the pegmatite body. The two anomalies PTc_1 and PTc_2 are aligned along the sheared zone. They are related to the presence of weak alteration product via kaolinization and ferrugination existing along the fracture of sheared pegmatite area. The dimensions of this anomaly are about 0.5m x 1.0m. The high values of radioactivity are due to the presence of primary uranium minerals.

Table 5. Statistical analysis of ground γ-ray Spectrometric survey of sheared pegmatite area.

	Total(Ur)	eU_{ppm}	eTh_{ppm}	eU/eTH	eTH/eU
Minimum:	9.4	1.90	5.70	0.09	1.17
25%-tile:	32.4	4.80	21.90	0.19	2.28
Median:	35.3	6.90	26.50	0.30	3.29
75%-tile:	38.3	10.5	32.10	0.44	5.36
Maximum:	212	91.8	208.4	0.86	11.61
Midrange:	110.7	46.8	107.1	0.47	6.39
Range:	202.6	89.9	202.7	0.77	10.44
Mean:	41.16	10.9	32.2	0.33	3.99
Standard Deviation:	28.91	13.5	28.3	0.17	2.25

Uranium distribution map of the sheared pegmatite

Generally, uranium mineralization is closely related to structural fissures. The distribution map of uranium shows that the uranium concentrations of the sheared pegmatite have three main anomalies enclosed between minimum 1.9 ppm of uranium and maximum 91.8 ppm with median 6.9 ppm uranium. These uranium anomalies, which represented by the contour lines more than 34 ppm (Fig. 19.B) are described as the following:

The anomaly PU_1 is related to the presence of alteration products as kaolinization and ferrugination, which exist along the fracture and the uranium minerals are easily visible by the naked eye (Fig. 3A) and picked from the mortared or brittle fragment by hand in the field. The minerals appear as black anhedral coarse grains, with submetalic luster. The data obtained from the Scan Electronic Microscope (EDAX) and XRD techniques show that the minerals are primary uranium. These minerals are surrounded by dark quartz and easily fractured to minute powdery fractions of clay minerals. The average eU content is more than 40ppm. The dimensions of this anomaly are 0.35m x 0.25m along the shear zone and present in two separate spots of about 45 and 75ppm. The second anomaly PU_2 lies in the western part of the shear zone and controlled by fractures and hematitization of the outer zone of the pegmatite body cutting by the shear zone. The eU content reaches more than 70ppm and extended about 1.0m. The same minerals of uranium and the mode of occurrences are the same as in PU_1 anomaly. The third anomaly PU_3 reaches up to 92ppm of eU and reaches to 1.5m in length, and is characterized by the presence of brownish yellow colour associated with the uranium minerals with glassy and translucent properties. The mineralogical study on this sample shows that the brownish yellow uranium mineral is liandratite coating the petscheckite grains.

Thorium distribution map of the sheared pegmatite

The thorium distribution contour map (Fig. 19C, Table 5) show that the area ranges between 5.7 ppm and 208.4 ppm with median 26.5 ppm of eTh. Some higher anomalies spots are recorded at the central part of the map within the sheared area, which bounded by the contour line 83 ppm. The first one PTh_1 is related to the area of uranium anomaly No. PU_1. It is bounded by the contour 145 ppm of eTh. The second anomaly PTh_2 is the highest and related the area of PU_2 anomaly of the shear zone. The eTh content in this anomaly reaches more than 251 ppm and controlled by fractures and alteration of the area around it. The third anomaly PTh_3 lies in the western part of the shear zone and controlled by fractures and hematitization of the wall rock of the pegmatite body, with the presence of argillic alteration which result from the bleaching out of the feldspars. The eTh content in this anomaly reaches more than 208 ppm and related to the uranium anomaly No. PU_3.

Relationship of eU/eTh and the presence of uranium mineralization

The presence of several spots exceeding 0.6 of eU/eTh ratios, greater than twice the average crustal eU/eTh ratios, are present in many parts along the sheared pegmatite zone. According to Charbonneau and Ford (1977) such an increase in equivalent uranium along with the increase in eU/eTh ratio may suggest a zone of uranium mineralization. By comparing the eU/eTh ratios map (Fig. 19.D) with the geologic map and the equivalent uranium contour map, it is noticed that the two anomalies No. P_1 and P_2 on figure 11.D are the best exposed for uranium mineralization as uraninite, brannerite, petscheckite and liandratite.....

Conclusions.

An elongated anomalous sheared pegmatite zone trending N 80° W is recorded within the monzogranite of El Regita area, south Sinai. It cuts through a zoned pegmatite body and has numerous altered spots dominated by hematitization and argillic materials as an indicator of wall-rock alterations. These spots contain high anomalous radioactive measurements generally associated with dark colour minerals which are picked and identified by XRD and ESEM techniques.

Laboratory investigations reveal the presence of uranium niobates, tantalates and titanates together with primary uranium mineralizations which are recorded for the first time in Sinai in the present work.

The uranium minerals include Brannerite, Petscheckite, liandratite, Uraninite, Pyrochlores, Betafite, Columbites and Ashanite. The high radioactive spots are subjected to ground gamma ray spectrometric measurements to determine the total counts, eU, eTh and K%. Four contour maps are constructed for those measured variables. The investigations of these maps reveal the presence of great resemblance between the total counts, eU and eTh radiometric contour maps which indicates that the total radioactivity of the area is generally ascribed to uranium and thorium–bearing minerals. Also, these high anomalous spots recorded on the contour maps are generally connected with altered spots recorded in the sheared pegmatite zone. Further work is required to understand and follow-up the form and setting of the uranium (ore) in subsurface zone.

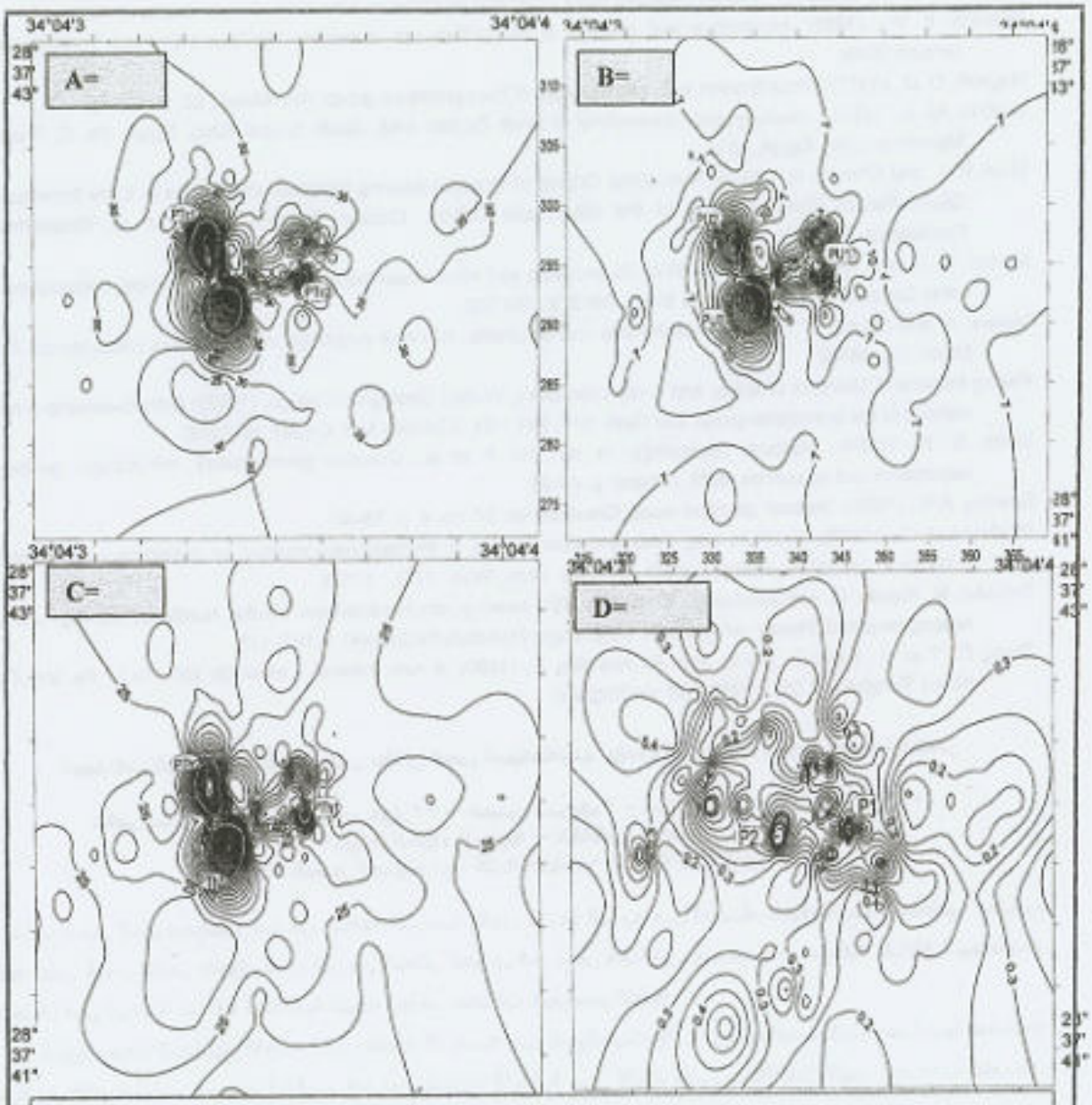

Fig. 11. Contour maps from ground γ-ray Spectrometric survey of sheared pegmatite area

REFERENCES

Bishr, A.H.A., (2007), Factors controlling mineralizations of some shear zones in granites, South Sinai, Egypt. Ph. D. Theses, Zagazig Univ., Zagazig. Egypt. 237p.

Charbonneau, B.W. and Ford, K.L., (1977): Uranium mineralization at the base of the Windsor Group, South Maitland, Nova Scotia; Current research, Part A, Geol. Surv. Can., Paper 78-1A, p. 419-425.

Dahlkamp, F. J., (1979): Uranlagerstätten, Gmelin Handbuch. Springer, Berlin Heidelberg New York, 280p.

El-Ghawaby, M. A., Hegazi, A. M., Khalifa, I. H. and Arnous, M. O., (2000): Tectonic and mineralization style of Saint Catherine Environs, south Sinai, Egypt. M.E.R.C. Ain Shams Univ., Earth Sci. Se. v. 14: p. 40-55.

Fayek, M., Utsunomiy, S., Ewing R., Riciputi, L., and Jensen, K. A., (2003): Oxygen isotopic composition of nano-scale uraninite at the Oklo-Okélobondo natural fission reactors, Gabon American Mineralogist, V. 88, p. 1583–1590.

Frondel, C., (1958): Systematic mineralogy of uranium and thorium, U. S. Geol. Surv. Bull 1064, 400p.

Gregory R. Lumpkin and Rodeny C. Ewing 2 (1996): Geochemical alteration of pyrochlore group minerals: Betafite subgroup. American Mineralogist, V. 81, p. 1237-1248.

Hawkes H. E. and Webb J.s., (1962): Geochemistry in mineral exploration. New York: Harper and row, 585 p.

Heinrich, E. W., (1958): Mineralogy and geology of radioactive raw materials, McGraw Hill, New York-Toronto-London, 654p.

Hogarth, D. D., (1977): Classification and nomenclature of the pyrochlore group. Am. Miner., 62, p. 403-10.

Ibrahim, M. E., (1991): Geology and radicactivity of Wadi Zaghra area, South central Sinai, Egypt. Ph. D. Thesis, Mansoura Univ., Egypt, 181p.

Mock R. L. and Ohmoto H. (1997): Nondetrital Origins of Uranium-bearing Minerals and Pyrites in Early Proterozoic Quartz-Pebble Conglomerates of the Elliot Lake District, Ontario. Seventh Annual V. M. Goldschmidt Conference. P. 2273.

Morton, R. D. and Sassano, G. P., (1972): Reflectance and micro indentation hardness vs chemical composition in some Canadian uraninites. N. Jb Miner, Mh 8, p. 350-360.

Mücke, A. and Strunz, H., (1978): Petscheckite and liandratite, two new pegmatite minerals from Madagascar, Am. Miner., 63, 941-6.

Peking Institute of Uranium Geology and X-ray Laboratory, Wuhan Geological College, (1978): Orthobrannerite-a new mineral of the brannerite group. Cta Geol. Sin., 241 – 51. (Chinese text; English abstract).

Smith, D. K., (1984): Uranium mineralogy, in: de Vivo F et al., Uranium geochemistry, mineralogy, geology, exploration and resources. IMM, London, p. 43-88.

Snelling, A.A., (1995): "Instant" petrified wood, Creation, vol. 17, no. 4, p. 38–40

Stuckless J. S., (1979): Uranium and thorium concentrations in Precambrian granites as indicators of a uranium province in central Wyoming. Contrib. Geology. Univ., Wyo., 17/2, 173-8.

Tomašić, N., Raade, G. and Bermanec, V., (2004): REE-bearing petscheckite from Tiltvika, Nordland, Norway, and its heating products. Neues Jahrbuch für Mineralogie Monatshefte 2004(4), p.163–175.

Zhang R., Tian H., Peng Z., Ma Z., Han F., and Jing Z., (1980): A new mineral – ashanite, (Nb, Ta,U, Fe, Mn)$_4$O$_8$. Kexue Tongbao, V. 25, p. 510–514. (in English).

تمعدنات اليورانيوم الأولية فى نطاق قص البيجماتيت بوادى الرقيطة, جنوب سيناء- مصر

عامر بشر*- سعيد ابو ضيف عزاز - حسن شريف* - ابراهيم الغطانى العاصى*-**
*** هيئة المواد النووية – القاهرة - مصر**
**** قسم الجيولوجيا- كلية العلوم- جامعة الزقازيق**

تكون صخور المونزوجرانيت جزء من منطقة الدراسة والتي تكتنف العديد من اجسام البيجماتيت الممنطق المتاثرة بوجود نطق القص والتى تحتوي على اثار من التحلل الجزئي في بعض المناطق. وجدت في منطقة تقاطع البيجماتيت مع نطاق قص الرجينة شادات اشعاعية نتيجة لتواجد تمعدنات اليورانيوم الاولية.

تتكون معادن اليورانيوم الاولية في منطقة الدراسة من اليورانينيت والبرانيريت والبتسكيت وتصاحبها تمعدنات اليورانيوم الثانوية الناشئة نتيجة التاكسد الجزئي للمعادن الاصلية مثل الاورثوبرانيريت واللياندرانيت. ويصاحب تمعدنات اليورانيوم معادن مصاحبة من الالمينيت اضافة الى الهيماتيت وبعض معادن الكاولينيت.

وجدت معادن اليورانيوم غنية بالعناصر الارضية النادرة مثل السريوم والنوديميم اضافة الى ذلك وجود تمعدنات اليورانيوم غنية بالنيوبيوم والتيتانيوم والتنتاليوم وهذا يوضح تكوينها بواسطة السوائل الحرمائية .